Journal of Alloys and Compounds 509 (2011) 5112–5118

Contents lists available at ScienceDirect

Journal of Alloys and Compounds

journal homepage: www.elsevier.com/locate/jallcom

Electrochemical and spectrophotometric study on neodymium ions in molten alkali chloride mixtures

Kazuhito Fukasawa[a,b,*], Akihiro Uehara[b], Takayuki Nagai[c], Toshiyuki Fujii[b], Hajimu Yamana[b]

[a] Graduate School of Engineering, Kyoto University, Katsura, Nishikyo-ku, Kyoto 615-8530, Japan
[b] Division of Nuclear Engineering Science, Research Reactor Institute, Kyoto University, 2-1010 Asashiro Nishi, Kumatori, Sennan, Osaka 590-0494, Japan
[c] Nuclear Fuel Cycle Engineering Lab., Japan Atomic Energy Agency, 4-33 Muramatsu, Tokai, Ibaraki 319-1194, Japan

ARTICLE INFO

Article history:
Received 30 September 2010
Received in revised form 25 January 2011
Accepted 27 January 2011
Available online 1 March 2011

Keywords:
Neodymium complex
Cyclic voltammetry
Absorption spectrophotometry
Molten salt
Alkali chloride
Gibbs free energy

ABSTRACT

The thermodynamic stability of Nd(III) complex in various molten alkali chlorides at 923 K was studied by electrochemical analysis. The standard Gibbs free energy change of the Nd^{3+} formation, $\Delta G^{\circ}_{3/0}$, decreased by adding MCl (M = Na, K, Rb, or Cs) into LiCl. The Nd(III) complex was more stable in an alkali chloride mixture with larger averaged cationic radius. This means that the stability is controlled by the polarizing power of solvent cations. The electronic absorption spectrum of the hypersensitive *f–f* transition of Nd^{3+} was investigated to know the change in its coordination environments. The oscillator strength of the $^4G_{5/2}$, $^2G_{7/2} \leftarrow {}^4I_{9/2}$ transition and the degree of the energy splitting in electronic energy levels were estimated. The results suggested that the octahedral symmetry of the $NdCl_6^{3-}$ complex was more distorted in the melt with higher LiCl content, and the distortion was depressed by decreasing the polarizing power of solvent cations. The local structure around Nd^{3+} was significantly correlated with the thermodynamic stability of the Nd(III) complex in molten alkali chlorides.

1. Introduction

The successful management of spent nuclear fuels is a key concern for the future stable utilization of nuclear power. Separation and transmutation of minor actinides (MA) such as Np, Am and Cm, are examined to minimize the amount of nuclear wastes as well as their long-lived radiotoxicities. Pyrochemical reprocessing using molten salts as a solvating medium has been proposed [1–7] due to some advantages for treating MAs, *e.g.*, high radiation and proliferation resistances of the process. In a typical pyrochemical reprocessing, spent nuclear fuels are dissolved in a molten salt and fuel materials are separated from fission products (FP) by electrodeposition or reductive extraction. To optimize the separation process, thermochemical properties of FPs and actinides in molten salt media are essential to be well understood.

Neodymium is one of major FP elements having larger neutron capture cross sections, and hence its removal in the pyrochemical reprocessing is desired. However, the reports for the electrochemical behavior of Nd in molten chlorides have been limited for LiCl–KCl [8–10], NaCl–$CaCl_2$ [9] and LiCl–$CaCl_2$ [10] eutectic melts. In order to assess the refining performance of Nd, systematic data for the chemical stability of Nd(III) complex in various alkali chlorides is necessary. Information on the coordination circumstance of solute ions is also important since it should be correlated with the stability. The predominant Nd(III) complex in molten alkali chlorides with low Nd^{3+} concentration has been confirmed to be $NdCl_6^{3-}$ with octahedral symmetry (O_h) by Raman spectrometry [11] and molecular dynamic simulation [12], respectively. The degree of the octahedral symmetry has been investigated for LiCl–CsCl mixtures employing absorption spectrum analysis, and the results reported that the $NdCl_6^{3-}$ complex was more distorted in the melts with lower CsCl content [13].

In the present study, the chemical stability and the coordination circumstances of the Nd(III) complex for various molten alkali chloride mixtures were investigated by electrochemical and absorption spectrum measurements, respectively. Their dependence on the melt compositions and the correlation between these macroscopic and microscopic properties were discussed.

2. Experimental

All experiments were carried out under an argon atmosphere, in which humidity and oxygen impurity were continuously kept less than 1 ppm. Anhydrous chlorides (99.99% purity) were purchased from Aldrich-APL LLC and used without further purification. 0.2–0.7 mol% $NdCl_3$ was dissolved in a quartz tube by various binary mixtures of alkali chlorides, LiCl–KCl, LiCl–NaCl, LiCl–RbCl and LiCl–CsCl.

An electrochemical measurement system Hz-5000 (Hokuto Denko Co.) was used for cyclic voltammetry (CV) and the differential pulse voltammetry (DPV). The sweep rate of CV for extracting peak potentials was 100 mV s^{-1}. The pulse height, period,

* Corresponding author at: Graduate School of Engineering, Kyoto University, Katsura, Nishikyo-ku, Kyoto 615-8530, Japan. Tel.: +81 724 51 2424; fax: +81 724 51 2634.
E-mail address: k.fukasawa@aw2.ecs.kyoto-u.ac.jp (K. Fukasawa).

0925-8388/$ – see front matter © 2011 Elsevier B.V. All rights reserved.
doi:10.1016/j.jallcom.2011.01.192

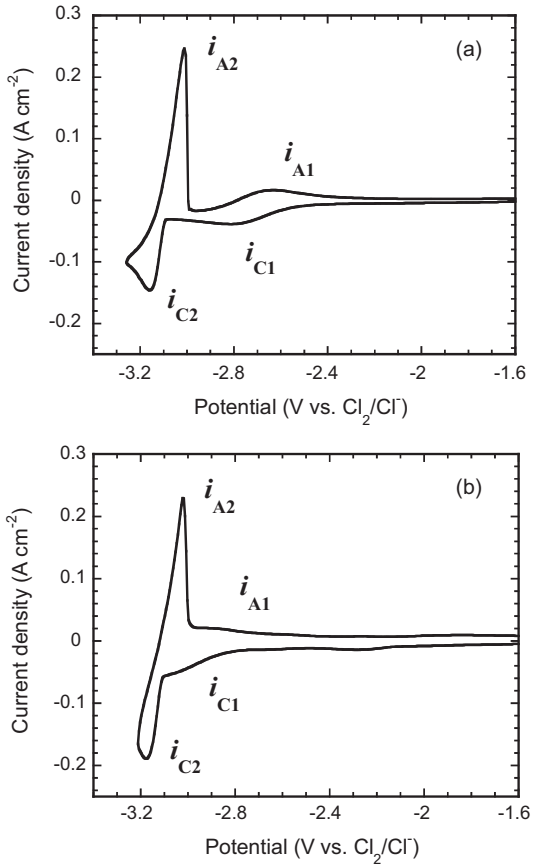

Fig. 1. Cyclic voltammograms of Nd in alkali chlorides at 923 K. Potential sweep rate of CV was 100 mV s^{-1}. (a) LiCl system. Mole fraction of $NdCl_3$ in LiCl was 0.60%. (b) LiCl–KCl eutectic system. Concentration of $NdCl_3$ in LiCl–KCl was 0.47%.

and width of DPV were 50 mV, 100 ms and 10 ms, respectively. A tungsten wire (99.95%, The Nilaco Co.) of 1 mm diameter, a pyrographite rod (99.99%, Tokai Carbon Co., Ltd.) of 3 mm diameter, and a Ag/Ag^+ electrode were used for the working, counter, and reference electrodes, respectively. In each measurement, the potential of chlorine gas evolution (Cl_2/Cl^-) on the pyrographite electrode [14] was determined to calibrate the Ag/Ag^+ electrode.

The electronic absorption spectra of Nd(III) in the melts were measured by using an UV/vis/NIR spectrometer (V-570, JASCO). The experimental apparatus was described in [15]. The analytical light from a light source (a tungsten halogen lamp) was guided to the electric furnace with quartz windows by using optical fibers, and the light passed through the sample in a quartz tube with a 10 mm light path inside the furnace. The light which traveled through the furnace was again guided to the spectrophotometer, in which a monochromator was set in front of detectors to decrease the background noise. The light intensity for the molten alkali chloride (I_0) and that including Nd(III) (I) was measured in the wavelength range of 300–850 nm at 0.5 nm intervals and 700–550 nm at 0.1 nm intervals. The absorbance was determined to be $-\log(I/I_0)$.

All the experiments were performed at 923 ± 3 K. In order to compare our results with reported data [9,16], the same experiment at different temperature, 723 ± 3 K, was also performed for a LiCl–KCl eutectic system.

3. Results and discussion

3.1. Determination of the standard potentials of the Nd^{3+} reduction

Typical cyclic voltammograms of Nd in LiCl and LiCl–KCl eutectic at 923 K are shown in Fig. 1. The electrochemical reduction process of Nd(III) in the eutectic has been identified to be a two-step process via Nd(II) by CV and chronopotentiometry [17],

$$Nd^{3+} + e^- \rightleftharpoons Nd^{2+} \quad (1)$$

$$Nd^{2+} + 2e^- \rightleftharpoons Nd^0\,(\text{metal}) \quad (2)$$

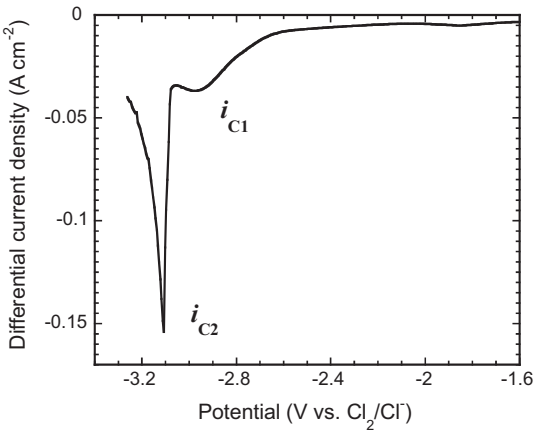

Fig. 2. Differential pulse voltammogram in LiCl–KCl eutectic melt at 923 K. Sweep rate of DPV was 50 mV s^{-1}. Concentration of $NdCl_3$ was 0.47 mol%.

The cathodic wave i_{C1} associated with an anodic wave i_{A1} is attributable to the soluble–soluble Nd^{3+}/Nd^{2+} couple. The cathodic peak i_{C2} associated with a sharp anodic peak i_{A2} corresponds to the Nd^{2+}/Nd^0 soluble–insoluble system. All peaks were separately observed for the LiCl system, where the cathodic peak currents were proportional to the square root of the potential sweep rate and the potential difference between positive and negative peak pairs were not significant. Hence both reactions were treated as reversible.

In the present study, the overlap of i_{C1} and i_{C2} in CV (Fig. 1b) was enhanced by adding MCl (M: Na, K, Rb, or Cs) into LiCl and it could not be resolved. In order to obtain sharp wave i_{C1}, the reduction reaction of Eq. (1) was analyzed by DPV. The result in the LiCl–KCl eutectic is shown in Fig. 2, in which the first peak was clearly obtained.

The following disproportionation reaction of Nd takes place in molten chlorides [8,9,18],

$$3Nd^{2+} \rightleftharpoons 2Nd^{3+} + Nd^0\,(\text{metal}) \quad (3)$$

It has been reported that the reaction is completed within several minutes [8]. This is much slower than the transient time during electrochemical measurement, and hence the interference of reaction 3 in our electrochemical analyses is considered to be insignificant.

The standard redox potential of the Nd^{3+}/Nd^{2+} couple, $E^\circ_{3/2}$, was determined by DPV as [19],

$$E^\circ_{3/2} = E_{\max} + \frac{\Delta E}{2} - \frac{RT}{F}\ln\left(\frac{D_{Nd^{2+}}}{D_{Nd^{3+}}}\right)^{1/2} - \frac{RT}{F}\ln\frac{\gamma_{Nd^{3+}}}{\gamma_{Nd^{2+}}} - E_{\text{ref}} \quad (4)$$

where $E_{\max}$, ΔE, and E_{ref} are the peak potential of i_{C1}, the applied potential pulse height, and the potential of the Ag/Ag^+ electrode vs. Cl_2/Cl^-, respectively. R is the gas constant, γ the activity coefficient, T the absolute temperature, and F the Faraday constant. The $E^\circ_{3/2}$ values were constant within the analytical uncertainty of ±10 mV in our experimental range from 0.2 mol% to 0.7 mol%. This means that the ratio of activity coefficients $\gamma_{Nd3+}/\gamma_{Nd2+}$ is constant and approximates that of diluted condition. Hence, $\gamma_{Nd3+}/\gamma_{Nd2+}$ set to be unity in the present study. D represents the diffusion coefficient of suffixed species. Due to the disproportionation reaction (Eq. (3)), it is impossible to measure an accurate diffusion property of Nd^{2+} and hence $D_{Nd^{2+}}$ is not available. In the present study, the ratio $D_{Eu^{2+}}/D_{Eu^{3+}}$ reported for europium [20] was substituted for $D_{Nd^{2+}}/D_{Nd^{3+}}$. The uncertainty of this substitution was examined to be small since both $D_{Ln^{2+}}$ and $D_{Ln^{3+}}$ decrease with the increase of atomic number and the decrease trends in lanthanide

Table 1
Standard redox potential in LiCl–KCl eutectic at 723 K.

Method		
CV	DPV	
$E^{\circ}_{3/2}$(V vs. Cl_2/Cl^-)		
−3.122 ± 0.010	−3.122 ± 0.010	[this study]
(−3.097)	(−3.097)	
−3.089 ± 0.001		[9]
−3.098 ± 0.010		[16]
$E^{\circ}_{2/0}$		
−3.142 ± 0.010		[this study]
−3.206 ± 0.003		[9]
−3.120 ± 0.015		[16]

series are monotonic: $D_{Ln^{2+}}$ is available for Sm, Eu, and Yb [21,22] for equimolar NaCl–KCl melt, and the evaluated $D_{Ln^{2+}}/D_{Ln^{3+}}$ values were similar, so that its variation resulted in an uncertainty < 2 mV on $E^{\circ}_{3/2}$. Moreover, the ratio $D_{Nd^{2+}}/D_{Nd^{3+}}$ for other molten chloride mixtures was assumed to be similar to the $D_{Eu^{2+}}/D_{Eu^{3+}}$ in equimolar NaCl–KCl melt that was equal to 1.96 [20].

The $E^{\circ}_{3/2}$ values obtained for the LiCl–KCl eutectic at 723 K are shown in Table 1. The $E^{\circ}_{3/2}$ values determined by DPV and convolution analysis of CV [19] agreed with each other. The literature values are shown together, in which $E^{\circ}_{3/2}$ was determined by the convolution analysis of CV and the D in the right side of Eq. (4) was not taken into account. We also determined $E^{\circ}_{3/2}$ following the same method that is shown in parenthesis. These values agreed with the literature values [9,16].

The standard redox potential of the Nd^{2+}/Nd^0 couple, $E^{\circ}_{2/0}$, was evaluated from CV as [23], which is available for reversible deposition reaction,

$$E^{\circ}_{2/0} = E_{pc} - \frac{RT}{nF}\ln \gamma_{Nd^{3+}} C_O + (0.9241)^2 \frac{RT}{nF} - E_{ref} \quad (5)$$

where E_{pc}, n, and C_O are the peak potential of CV cathodic peak i_{C2}, the reaction electron number (n = 2, in the present case), and the bulk concentration, respectively. The $E^{\circ}_{2/0}$ values were proportional to the natural logarithm of $NdCl_3$ concentration in the measured range, which is another indication to assume γ is equal to unity in this study. The obtained $E^{\circ}_{2/0}$ values shown in Table 1 are consistent with the literature data [16].

It should be noted that, in this section, we used the Cl_2/Cl^- equilibrium potential determined by using a chlorine gas electrode [24] in order to obtain the precise standard potential values. In following sections, the Cl_2 evolution potential mentioned in experimental section will be used as the standard redox potential of the Cl_2/Cl^- couple, E_{ref} in Eqs. (4) and (5). Though the Cl_2 evolution potential slightly shifts from the Cl_2/Cl^- equilibrium potential, the former method is feasible for systematic study with molten salts of various components.

3.2. Dependence of the standard Gibbs free energy change of the Nd(III) formation on the melt composition

The standard redox potential of the Nd^{3+}/Nd^0 couple, $E^{\circ}_{3/0}$, was calculated from $E^{\circ}_{3/2}$ and $E^{\circ}_{2/0}$ by employing the following equation,

$$E^{\circ}_{3/0} = \frac{E^{\circ}_{3/2} + 2E^{\circ}_{2/0}}{3} \quad (6)$$

The standard Gibbs free energy change of Nd^{3+} formation, $\Delta G^{\circ}_{3/0}$, was derived as,

$$\Delta G^{\circ}_{3/0} = nFE^{\circ}_{3/0} \quad (7)$$

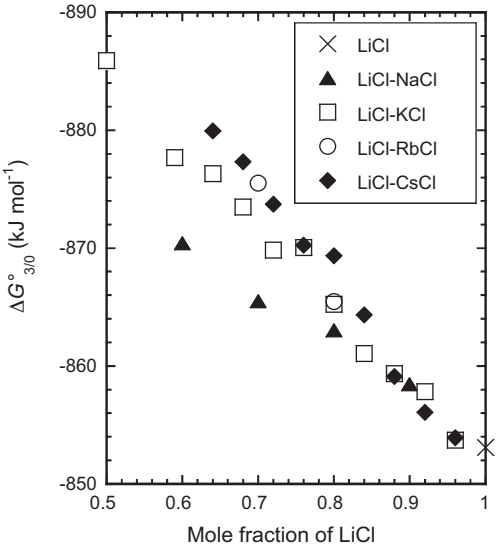

Fig. 3. Dependence of standard Gibbs free energy change of Nd^{3+} formation on melt compositions.

The reaction corresponding to the $\Delta G^{\circ}_{3/0}$ is given as the following reaction.

$$Nd(s) + 3/2Cl_2(g) + 3Cl^-(solution) \rightleftharpoons NdCl_6{}^{3-}(solution) \quad (8)$$

The $\Delta G^{\circ}_{3/0}$ values were evaluated for various binary mixtures of alkali chloride MCl (M: Na, K, Rb, or Cs) and LiCl at 973 K. It should be noted that we do not assume Cl_2/Cl^- couple as an absolute reference, which means the activity of Cl^- is not invariable for the melt compositions. The melt composition changes the chemical status of both Cl^-(solution) and $NdCl_6{}^{3-}$(solution). As defined in the above reaction, the observed $\Delta G^{\circ}_{3/0}$ values represent the difference between the Gibbs energy levels of these two.

Fig. 3 shows $\Delta G^{\circ}_{3/0}$ obtained as function of LiCl content. The maximum mole fraction of MCl was limited by following two reasons: (1) melting point of the sample and (2) cathode limit (Alkali metal deposition) for electrochemical analysis. The $\Delta G^{\circ}_{3/0}$ value increased by adding MCl into LiCl, which means that the addition of MCl makes the Nd(III) complex stable. In alkali cation series, the ionic radius is in the order of $Li^+ < Na^+ < K^+ < Rb^+ < Cs^+$, and the polar-

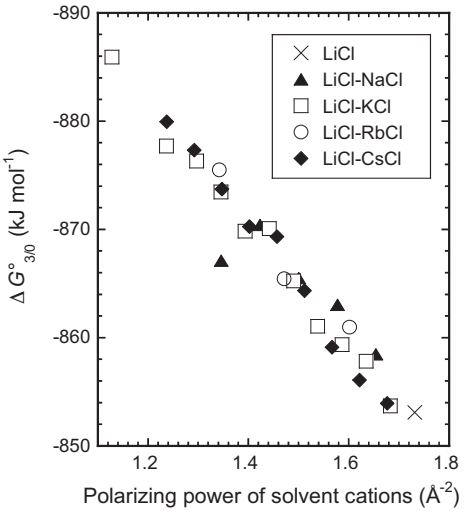

Fig. 4. Dependence of standard Gibbs free energy change of Nd^{3+} formation on polarizing power of solvent cations.

Table 2
Ionic radius and polarizing power of cations.

	Ionic radius r/Å [26]	Polarizing power P[a]
Li^+	0.76	1.73
Na^+	1.02	0.96
K^+	1.38	0.53
Rb^+	1.52	0.43
Cs^+	1.67	0.36
Nd^{3+}	1.36	1.62

[a] See Eq. (10).

izing ability is in the inverse order. That is, the alkali cation with smaller ionic radius like Li^+ interacts with Cl^- strongly. Hence, there could be strong interaction among Li^+ and chloride ions coordinating to the solute Nd^{3+} in LiCl.

For mixtures of alkali chlorides, the polarizing ability of alkali cations to Cl^- could be an average of each according to the mixing ratio. Redox potential of some chemical reactions in molten salts was reported to be correlated with the "charge density",

$$M = \sum n_i \frac{z_i}{r_i^3} \tag{9}$$

where n_i is the molar fraction of the ith component with the cation of radius r_i having a charge of z_i [25,26]. However, they counted solute ion as a component as well as solvent ions and in general, the ionic potential z/r, or the force z/r^2 is more rational than M as an expression of polarizing ability of solvent alkali cations.

In this study, we found that $\Delta G^\circ_{3/0}$ has a strong correlation with the averaged "polarizing power" of alkali cations in the melts,

$$P = \sum n_i \frac{z_i}{r_i^2} \tag{10}$$

Ionic radius r_i for six coordinated ions [27] was used in the present study. The r_i and P_i values are shown in Table 2. The relationship between $\Delta G^\circ_{3/0}$ and P is shown in Fig. 4. The relation between $\Delta G^\circ_{3/0}$ and P can be expressed by linear functions for all alkali binary mixtures. The Nd(III) complex is more stable in the alkali binary mixture with smaller polarizing power, and the stability increases with a constant slope, $\delta(\Delta G^\circ_{3/0})/\delta P$.

3.3. Coordination environment of $NdCl_6^{3-}$

Absorption spectra of Nd^{3+} in molten LiCl–NaCl, LiCl–KCl, LiCl–RbCl and LiCl–CsCl mixtures and LiCl at 923 K were measured.

A typical absorption spectrum of Nd^{3+} in the LiCl–KCl eutectic is shown in Fig. 5, in which an intensive absorption peak can be seen at 589 nm. This peak is assigned to be the f–f transitions

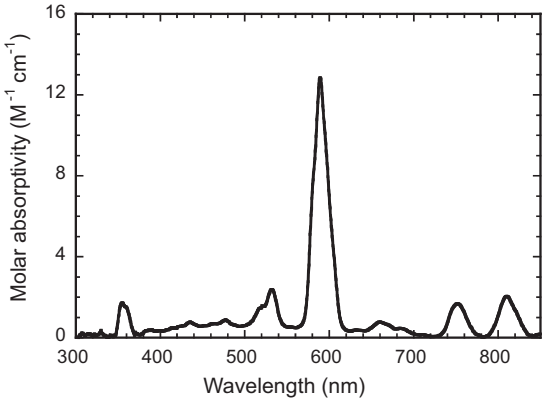

Fig. 5. Absorption spectra of Nd^{3+} in LiCl–KCl eutectic melt.

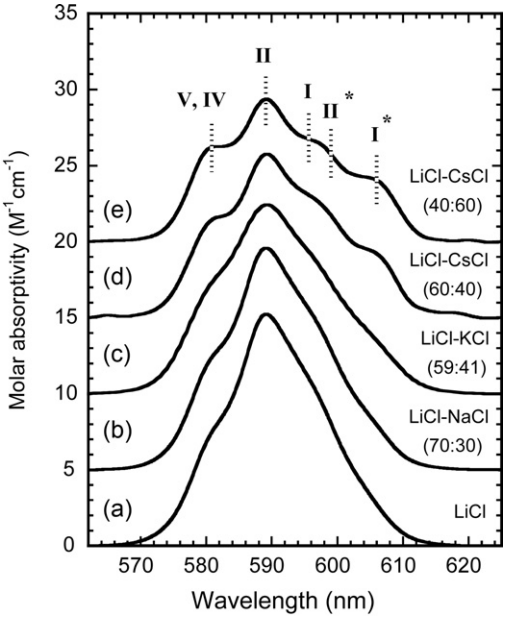

Fig. 6. Electronic absorption spectra of Nd^{3+} in molten alkali chlorides at 973 K. (a) LiCl system. (b) 70 mol% LiCl and 30 mol% NaCl system. (c) LiCl–KCl eutectic system. (d) 60 mol% LiCl and 40 mol% CsCl system. (e) 40 mol% LiCl and 60 mol% CsCl system.

from the ground level $^4I_{9/2}$ to the excited levels of $^4G_{5/2}$ and $^2G_{7/2}$. The $^4G_{5/2} \leftarrow {}^4I_{9/2}$ transition, which is known as the hypersensitive f–f transitions, is sensitive to changes in the coordination circumstance and commonly used to examine the complexation of Nd^{3+} in solutions [13]. Fig. 6 shows the absorption spectra of $^4G_{5/2}$, $^2G_{7/2} \leftarrow {}^4I_{9/2}$ transition for LiCl and some binary alkali chlorides, ranging from 562 to 625 nm wavelength. The spectra are composed of several transitions between split degenerate terms of the ground and excited levels. The transitions between the split degenerate states are schematically shown in Fig. 7. According to the reported energy diagram [13], each transition shown in Fig. 6 was assigned. The spectrum peaks corresponding to each transition were separable using Gaussian functions, and consequently, wave numbers at each peak position were determined.

The electric field given by the symmetrical octahedral coordination of $NdCl_6^{3-}$ promotes the splitting of the degenerate energy states, which makes the absorption peaks separable as the LiCl–CsCl system (spectrum (e) in Fig. 6). In the same manner, sharper absorption spectrum as the LiCl case (spectrum (a) in Fig. 6) where the energy splitting is depressed indicates that the symmetry of $NdCl_6^{3-}$ is distorted in the melt. As shown in Figs. 6 and 7, the difference of peak positions I* and II is equal to the sum of energy

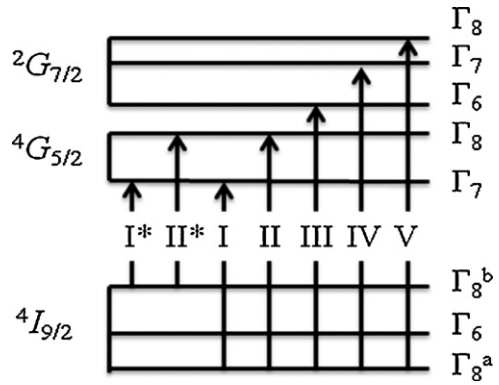

Fig. 7. Diagram of hypersensitive transitions of $NdCl_6^{3-}$. The diagram was quoted from the literature [13].

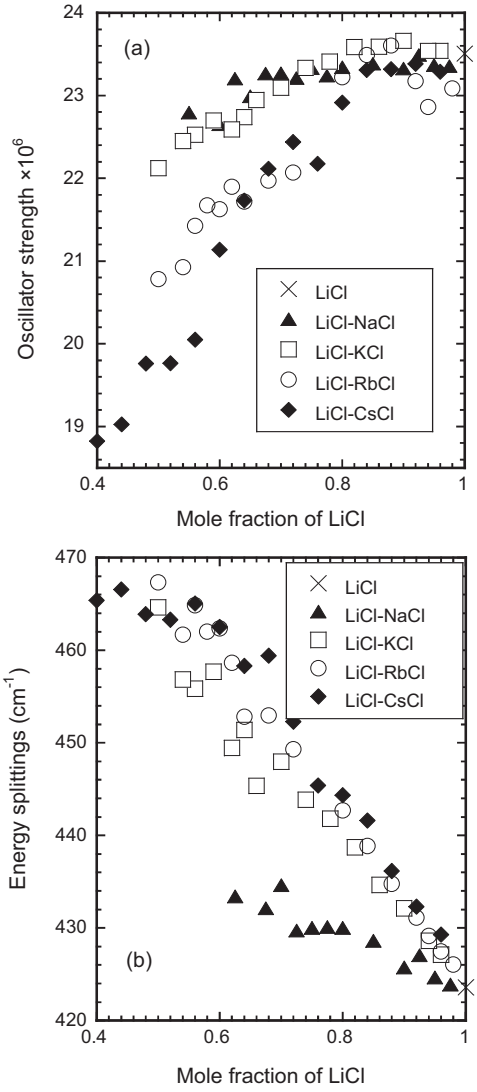

Fig. 8. Dependence of oscillator strength and splitting energy of hypersensitive transition of Nd^{3+} on melt compositions. (a) Oscillator strength. (b) Splitting energy.

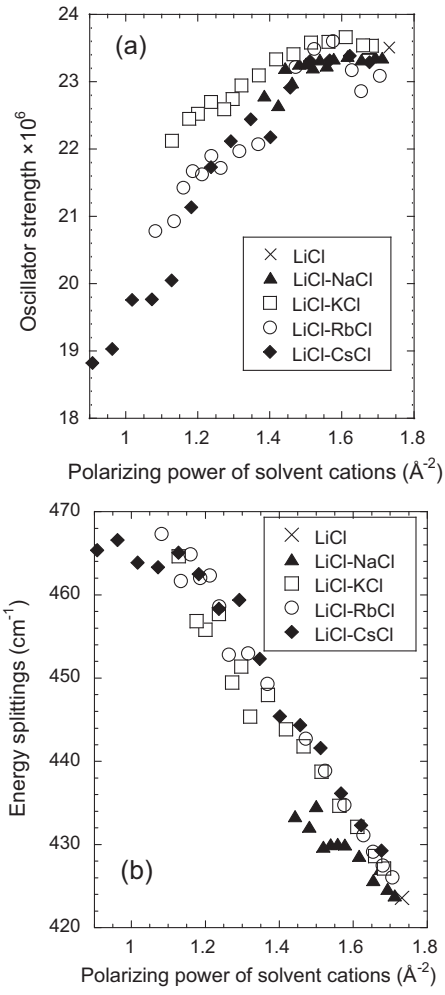

Fig. 9. Dependence of oscillator strength and splitting energy of hypersensitive transition of Nd^{3+} on polarizing power of solvent cations. (a) Oscillator strength. (b) Splitting energy.

splitting of the $^4I_{9/2}$ and $^4G_{5/2}$ states, $\Sigma\Delta E$, and hence the term of $\Sigma\Delta E$ is a useful probe to know the symmetry of $NdCl_6^{3-}$ [13].

The transition probability of the $^4G_{5/2}$, $^2G_{7/2} \leftarrow {}^4I_{9/2}$ transition, which is expressed as the oscillator strength, also gives information of the coordination circumstance $NdCl_6^{3-}$. Oscillator strength f is defined as,

$$f = 4.319 \times 10^{-9} \frac{9n}{(n^2+2)^2} \int \varepsilon(\upsilon) d\upsilon \qquad (11)$$

where $\varepsilon(\nu)$ is the molar absorptivity at energy $\nu(\mathrm{cm}^{-1})$ and n is the reflective index of the solvent medium. $\varepsilon(\nu)$ was integrated from 562 to 625 nm in the present study. The reflective indexes of single alkali chlorides are available [28]. For binary mixtures, the n value was estimated by a linear interpolation between the values of pure component melts [29]. Table 3 shows the oscillator strengths, $\Sigma\Delta E$, and molar absorptivities at 589 nm for binary eutectics.

The f and $\Sigma\Delta E$ values for binary alkali chlorides obtained are shown in Fig. 8 as functions of LiCl mole fraction, χ_{LiCl}. $\Sigma\Delta E$ decreased with the increase of χ_{LiCl}, which suggests the distortion of the octahedral symmetry of $NdCl_6^{3-}$. The f values increased with χ_{LiCl}, and this also suggests the distortion proceeds. Our results showed a similar trend reported for $NdCl_3$ in $LaCl_3$–KCl mixtures [30].

Fig. 9 shows the dependence of f and $\Sigma\Delta E$ on the polarizing power of solvent cations, P. The f values increased with P, while $\Sigma\Delta E$ linearly decreased with the increase of P. Different MCl–LiCl systems show different increasing rates of f (Fig. 9a), while the

Table 3
Sum of splitting of electronic energy levels, molar absorptivity at 589 nm, and the oscillator strength of hypersensitive transitions.

Spectrum	Medium (molar ratio)	ε_{589} (M^{-1} cm^{-1})	$f(\times 10^6)$	$\Sigma(\Delta E)^a$ (cm^{-1})
(a)	LiCl	15.2	23.5	421
(b)	LiCl–NaCl (70:30)	14.5	23.2	432
(c)	LiCl–KCl (59:41)	12.4	23.1	454
(d)	LiCl–CsCl (60:40)	10.7	21.1	460
(e)	LiCl–CsCl (40:60)	9.35	18.8	463

$\Delta E(^4I_{9/2}) + \Delta E(^4G_{5/2})$. Peak positions were analyzed by dividing the raw spectrum into four simple Gaussian functions.

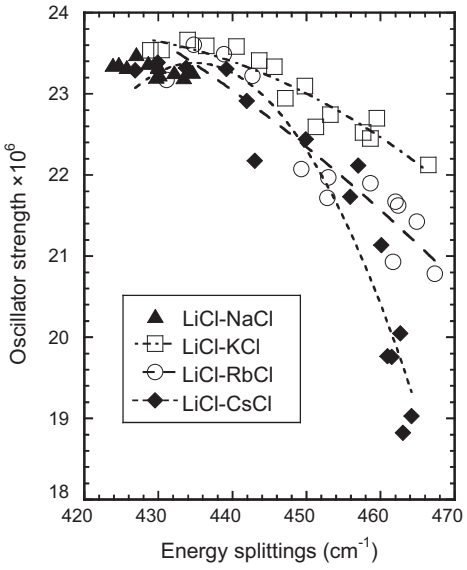

Fig. 10. Dependence of oscillator strength on energy splitting. Dashed, dashed-dotted and dashed-two dotted lines are quadratic approximated curves of dots for LiCl–KCl, LiCl–RbCl and LiCl–CsCl systems, respectively.

decreasing rates and absolute values of $\Sigma\Delta E$ are similar for all MCl–LiCl systems (Fig. 9b). The factors influencing f in molten alkali chlorides are: (a) the distortions from octahedral symmetry, and, (b) the electron donating ability of the chloride anion [31]. Fig. 9b suggests that $\Sigma\Delta E$ correlated with the factor (a) [13], is simply controlled by P for molten alkali chloride systems. On the other hand, f varies for different MCl–LiCl systems at the low χ_{LiCl} region, which suggests that the factor (b) is also important.

Fig. 10 shows f as a function of $\Sigma\Delta E$. The f value similarly decreased with the increase of $\Sigma\Delta E$ in every mixtures near $\chi_{Li} = 1$, but it was clearly different depending on the mixed cations in the region of higher $\Sigma\Delta E$; the f value was smaller in the sequence of $K^+ \rightarrow Cs^+$. These cations have lower polarizing power that enlarges the electron donating ability of Cl^- in the same sequence. This suggests that the effect of factor (b) gradually emerges at the low χ_{LiCl} region.

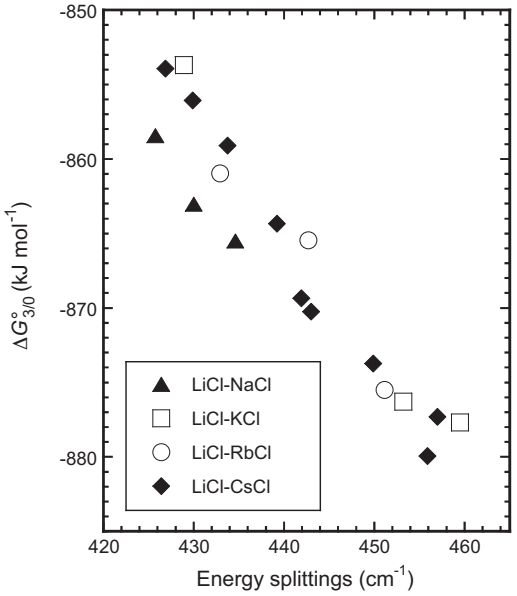

Fig. 11. Relationship between standard Gibbs free energy change of Nd^{3+} formation and energy splittings.

The discussion above is also suggestive that the local structure around Nd^{3+} significantly correlates with the bulk thermodynamic stability since both $\Sigma\Delta E$ and $\Delta G^\circ_{3/0}$ depend well upon P. Fig. 11 shows the relationship between $\Sigma\Delta E$ and $\Delta G^\circ_{3/0}$ in which $\Delta G^\circ_{3/0}$ decreases with increase of $\Sigma\Delta E$. From these results, we can conclude that the polarizing power of solvent cations controls the degree of distortion from octahedral symmetry of ligand chloride structure which is correlated with the thermodynamic stability of $NdCl_6^{3-}$ complex in molten alkali chlorides.

4. Conclusion

The $\Delta G^\circ_{3/0}$ value decreased by adding MCl (M = Na, K, Rb, or Cs) into LiCl. This means that the Nd(III) complex is more stable in the alkali chloride mixture with larger averaged cationic radius. $\Delta G^\circ_{3/0}$ is correlated with the polarizing power of solvent cations.

The change in the oscillator strength of the $^4G_{5/2}$, $^2G_{7/2} \leftarrow {}^4I_{9/2}$ transition and the degree of the energy splitting in electronic energy levels suggested that the octahedral symmetry of the $NdCl_6^{3-}$ complex is more distorted in the melts of higher LiCl content. The degree of distortion is correlated with increasing the polarizing power of solvent cations.

The polarizing power of solvent cations controls the local structure around Nd^{3+} and the degree of its distortion from octahedral symmetry is correlated with thermodynamic stability of $NdCl_6^{3-}$ complex in molten alkali chlorides.

Acknowledgement

The authors are grateful to Mr. Roy Jacobus for his help in improving the English expressions of this paper.

References

[1] Y.I. Chang, Nucl. Technol. 88 (1989) 129.
[2] K. Uozumi, M. Iizuka, T. Kato, T. Inoue, O. Shirai, T. Iwai, Y. Arai, J. Nucl. Mater. 325 (2004) 34.
[3] T. Koyama, M. Iizuka, Y. Shoji, R. Fujita, H. Tanaka, T. Kobayashi, M. Tokiwai, J. Nucl. Sci. Technol. 34 (1997) 384.
[4] M. Iizuka, K. Uozumi, T. Inoue, T. Iwai, O. Shirai, Y. Arai, J. Nucl. Mater. 299 (2007) 32.
[5] Z. Tomczuk, J.P. Ackerman, R.D. Wolson, W.E. Miller, J. Electrochem. Soc. 139 (12) (1992) 3523.
[6] O. Conocar, N. Douyere, J.P. Glatz, J. Lacquement, R. Malmbeck, J. Serp, Nucl. Sci. Eng. 153 (2006) 253.
[7] J.J. Roy, L.F. Grantham, D.L. Grimmett, S.P. Fusselman, C.L. Kruger, T.S. Storvick, T. Inoue, Y. Sakamura, N. Takahashi, J. Electrochem. Soc. 143 (8) (1996) 2487.
[8] H. Yamana, B.G. Park, O. Shirai, T. Fujii, A. Uehara, H. Moriyama, J. Alloys Compd. 408–412 (2006) 66.
[9] Y. Castrillejo, M.R. Bermejo, E. Barrado, A.M. Martinez, P.D. Arocas, J. Electroanal. Chem. 545 (2003) 141.
[10] K. Fukasawa, A. Uehara, T. Nagai, T. Fujii, H. Yamana, Proceedings of 1st International Symposium Kyoto University Global COE Program - Zero Carbon Kyoto 2009, Kyoto, Japan, August 20, 2009, p. 330.
[11] Yu.A. Barbanel, V.V. Kolin, V.P. Kotlin, A.A. Lumpov, J. Radioanal. Nucl. Chem. 143 (1990) 167.
[12] G.M. Photiadis, B. Borresen, G.N. Papatheodorou, J. Chem. Soc. Faraday Trans. 94 (1998) 2605.
[13] T. Fujii, T. Nagai, N. Sato, O. Shirai, H. Yamana, J. Alloys Compd. 393 (2005) L1–L5.
[14] T. Murakami, T. Nohira, Y.H. Ogata, Y. Ito, Electrochem. Solid State Lett. 8 (1) (2005) E1–E3.
[15] T. Nagai, T. Fujii, O. Shirai, H. Yamana, J. Nucl. Sci. Technol. 41 (6) (2004) 690.
[16] Y. Motto, Doctoral Thesis, Paris, 1986.
[17] R. Bermejo, Y. Castrillejo, A. Martínez, E. Barrado, Proceedings of GLOBAL2001, Paris, France, September 13, 2001.
[18] H. Hayashi, M. Akabori, T. Ogawa, K. Minato, Z. Naturforsch. 59a (2004) 705.
[19] A.J. Bard, L.R. Faulkner, Electrochem. Meth., 2nd ed., Wiley, New York, 2001.
[20] S.A. Kuznetsov, M. Gaune-Escard, Electrochim. Acta 46 (2001) 1101.
[21] S.A. Kuznetsov, M. Gaune-Escard, J. Electroanal. Chem. 595 (2006) 11.
[22] S.A. Kuznetsov, M. Gaune-Escard, Proceedings of the 7th International Symposium on Molten Salts Chemistry and Technology MS 7, Toulouse, France, August 29–September 2, 2005, p. 855.

[23] T. Berzins, P. Delahay, J. Am. Chem. Soc. 75 (1953) 555.
[24] O. Shirai, T. Nagai, A. Uehara, H. Yamana, J. Alloys Compd. 456 (2008) 498.
[25] G.W. Mellors, S. Senderoff, J. Electrochem. Soc. 108 (1) (1961) 93.
[26] H.C. Gaur, H.L. Jindal, Electrochim. Acta 15 (1970) 1127.
[27] R.D. Shannon, Acta Crystallogr. A32 (1976) 751.
[28] Y. Iwadate, J. Mochinaga, K. Kawamura, J. Phys. Chem. 85 (1981) 3708.
[29] M. Matsuura, H. Maruta, Y. Kuroki, Electrochemistry 73 (8) (2005) 573.
[30] A. Chrissanthopoulos, G.N. Papatheodorou, J. Mol. Struct. 782 (2006) 130.
[31] A. Chrissanthopoulos, G.N. Papatheodorou, Phys. Chem. Chem. Phys. 2 (2000) 3709.